JOURNAL OF MATERIALS SCIENCE 24 (1989) 2214–2220

Improvement in colloidal sol–gel SiO_2 glass by attrition of aggregates in sols

D. W. JOHNSON, Jr, E. M. RABINOVICH, D. A. FLEMING, J. B. MacCHESNEY
AT&T Bell Laboratories, Murray Hill, New Jersey 07974, USA

The two-step colloidal sol–gel process for forming SiO_2 glasses has been improved by the use of attrition in ball mills consisting of borosilicate glass jars with fused SiO_2 cylinders as milling media. The average size of aggregates was reduced from more than 40 μm to less than 3 μm by milling up to 64 h depending on the hardness of the dried gel. Data on pore size distribution in the twice dispersed and dried gels show that 24 to 30 vol% of the pores are due to interaggregate spaces (pores whose sizes are larger than those represented by the average 16 nm pores between primary SiO_2 particles). These large pores cause a bimodal size distribution with the secondary peak at 3 to 4 μm with no milling and the position of the secondary peak decreases with milling until it is no longer resolved from the primary peak. The average size of the interaggregate pores is more than an order of magnitude smaller than the average size of the aggregates due to the efficiency of packing the aggregates of a broad size distribution. Milling is shown to markedly improve the transparency of the SiO_2 glass after sintering.

1. Introduction

Preparation of high silica glass articles by sol–gel methods are categorized into two major areas: those utilizing the hydrolysis and polymerization of silicon organometallics such as tetraethylorthosilicate to form monolithic gel shapes which are subsequently dried and sintered; and those utilizing colloidal sols where finely divided high silica particles are dispersed into a sol, the sol is gelled, dried and sintered into a glass. The monolithic alkoxide route has been extensively studied and reviewed elsewhere [1, 2]. The method has the advantages of producing a dried gel with uniform small pores permitting sintering at low temperatures and offers the flexibility of uniformly incorporating some dopant and modifier ions into the glass. However, the method does suffer from large drying shrinkages which easily crack large monolithic pieces of gel unless the drying takes place very slowly; perhaps over the course of weeks or months.

A form of colloidal sol–gel for high silica glasses was first reported by Shoup [3] where alkali stabilized silica sols were gelled and leached free of alkali before sintering into shapes. The use of pure SiO_2 to form aqueous colloidal sols which would gel, dry and sinter has been reported from these laboratories [4–6]. Subsequently, Scherer and Luong [7] reported a similar method based on non-aqueous sols.

The early experiments with colloidal dispersions of silica in water used fumed silica (made by the flame hydrolysis of silicon tetrachloride) which was dispersed in water using a shear mixer such as a common blender. These sols were uniform and were found to gel by a hydrogen bonding mechanism [8]. However, the drying shrinkage was large enough that shapes could be successfully dried only using slow drying or by drying in a humidity chamber where high humidity prevented large gradients in water contents. A major improvement was made when it was found that by merely drying this first gel quickly and redispersing the fragments in water again using a shear mixer, the resultant sol (twice dispersed) had a rheology similar to the previous sol but had markedly less drying shrinkage and thus could be dried faster; in the order of 1 to 2 days [4]. The lesser shrinkage is due to a sol structure consisting of aggregates of SiO_2 particles large enough to interlock on gelation and prevent excessive shrinkage [4, 5]. The interstices between the aggregates were also larger than those between the ultimate particles and served to allow more rapid transport of the water to the surface during drying.

It was also found that by heating the first dispersed gel to temperatures as high as 1000° C, improvement in the quality of sintered glass would be attained [4]. For temperatures up to 900° C, little or no change in surface area was detected indicating minimal sintering but the friability of the heat treated gels did decrease with temperature indicating at least some neck formation.

While the large interaggregate porosity is advantageous in allowing transport of water during drying of the gel and allowing reactant gases such as chlorine to diffuse in prior to sintering, it had been noted that excessively large pores could serve as areas which would sinter more slowly than the denser surroundings and in some cases remain as voids in the sintered glass. For some applications these microvoids may be of no consequence but for an application such as optical fibres (lightguides) such defects cannot be tolerated. The purpose of the work reported here is to examine methods for controlling the size of aggregates

0022–2461/89 $03.00 + .12

and measure the effects of aggregate size on pore size distributions and the quality of sintered SiO_2 glass. The method chosen to reduce the size of the aggregates in the second sol is essentially classical ball milling. As impurities imparted by attrition of traditional ceramic mills and milling media cause crystallization of high SiO_2 glasses during sintering or defects in sintered glass, high purity glass jars and milling media were used.

It has been recognized that the distribution of aggregates obtained in the twice dispersed gels is advantageous in minimizing shrinkage during drying and in allowing larger transport paths for water during drying or for infusion of reactant gases prior to sintering [4, 5]. This work shows that by reducing the size of the aggregates in the second sol using comminution, the additional microstructural uniformity can improve the quality of the sintered glass. The work also seeks to quantify the effects of such comminution on the sol and determine optimal conditions for processing of colloidal sol–gel glasses.

2. Experimental Procedure

Fumed SiO_2* of specific surface area $\sim 200\,m^2\,g^{-1}$ was dispersed in water at a loading of 29 wt % using a blender as described earlier [4]. This sol was then dried at 150° C in loosely covered containers yielding irregular fragments of dried gel from a few millimetres to a few centimetres in size. For some experiments, this material was used directly for subsequent processing and is designated as 150° C material. For other experiments the dried fragments were heat treated at 900° C for 4 h in covered vitreous SiO_2 containers and designated as 900° C material. This temperature was chosen because it contrasted with the 150° C material in difficulty of breaking the aggregates. In both cases the specific surface area remained at about $200\,m^2\,g^{-1}$.

The dried aggregates were further processed into twice dispersed sols by blending the material with water for about 2 min at a loading rate of 36 wt % SiO_2 in water. For experiments where no further attrition was desired, this sol was poured into SiO_2 mould tubes ranging in diameter from 11 to 25 mm, allowed to gel overnight in the closed moulds and then removed from the moulds for drying. Drying was accomplished by allowing the parts to stand in the ambient laboratory conditions.

Further attrition of the blended sols was accomplished by ball milling. For this, borosilicate jars were used with fused SiO_2 milling media prepared by cutting 12 mm diameter SiO_2 rods into approximately 12 mm lengths. These short cylinders were rotated with abrasive powder for several days to round the edges. The jars containing the sol and milling media were rotated at about 90 r.p.m. for times of 1, 2, 4, 8, 16, 32 and 64 h after which rods were cast and dried as described above.

Aggregate size distributions in the twice dispersed sols were characterized using an electrozone sensing apparatus†. A few drops of the concentrated sol were mixed with 50 ml of water and a few drops of this diluted slurry were added to 200 ml of 1% NaCl solution in the electrozone sensor. Aperture sizes ranging from 30 to 200 μm were used for the measurement depending on the size of the aggregates. Therefore the minimum detectable size was 0.5 μm.

The pore structure of the dried gels was characterized using a mercury porosimeter‡. The drying shrinkages of these twice dispersed gels were not measured directly but it was noted that the degree of milling does affect the drying shrinkage. The linear percentage drying shrinkages were calculated from the initial density of SiO_2 in the sol (known from the SiO_2 to H_2O ratios) and the bulk density of the dried gels as measured by mercury porosimetry. It is known that the volume change on gelation is very small in these systems and is here assumed to be zero. For this calculation

$$\frac{\Delta L}{L} = 1 - \left(\frac{\varrho_i}{\varrho_f}\right)^{1/3}$$

where ΔL is the length change on drying, L the undried length, ϱ_i is the initial density of SiO_2 in the sol and ϱ_f is the final bulk density of the dried gel.

Sintering of dried gels was done by first dehydrating in Cl_2 + He at 1000° C for 2 to 6 h and then heating to 1300 to 1450° C in pure helium.

3. Results

Fig. 1 shows a typical aggregate size distribution. For this measurement, a 30 μm orifice was used and the peak of the aggregate size distribution is at about 2.5 to 3 μm. This peak position was used to characterize the aggregate size. Peak positions measured for samples of both the 150 and 900° C dried materials milled at various times are shown in Fig. 2. The sol prepared from the once dispersed gel dried at 150° C could not be milled for 32 h or more because with the longer milling times the sol would increase in viscosity, the milling media would adhere to the walls of the jar and then in the absence of ball movement the sol would gel into a semirigid mass.

The pore size distribution of 900° C material milled for 8 h is shown in Fig. 3. The smaller peak at the larger pore sizes (referred to here as the secondary peak) was uniquely resolved for the 900° C samples milled for all but the 32 and 64 h whereas the peak was resolved only for the unmilled sol prepared from the 150° C material. The pore diameters at the peak positions of these secondary peaks are shown in Fig. 4 as a function of milling time.

From the pore size distribution data, the fraction of total porosity whose diameters are larger than 1 μm, 100 nm, 50 nm, 30 nm and larger than the position of the major peak (or primary peak) at about 10 to 16 nm was calculated. These data are shown in Fig. 5a for the 150° C material and in Fig. 5b for the 900° C material. Note that the volume fraction of pores whose size

*Cab-O-Sil, M-5, Cabot Corp., Tuscola, Ill., USA.
†Coulter Counter, Model T, Coulter Electronics Corp.
‡Micromeretics Auto Pore 9200, Micrometeretics Corp.

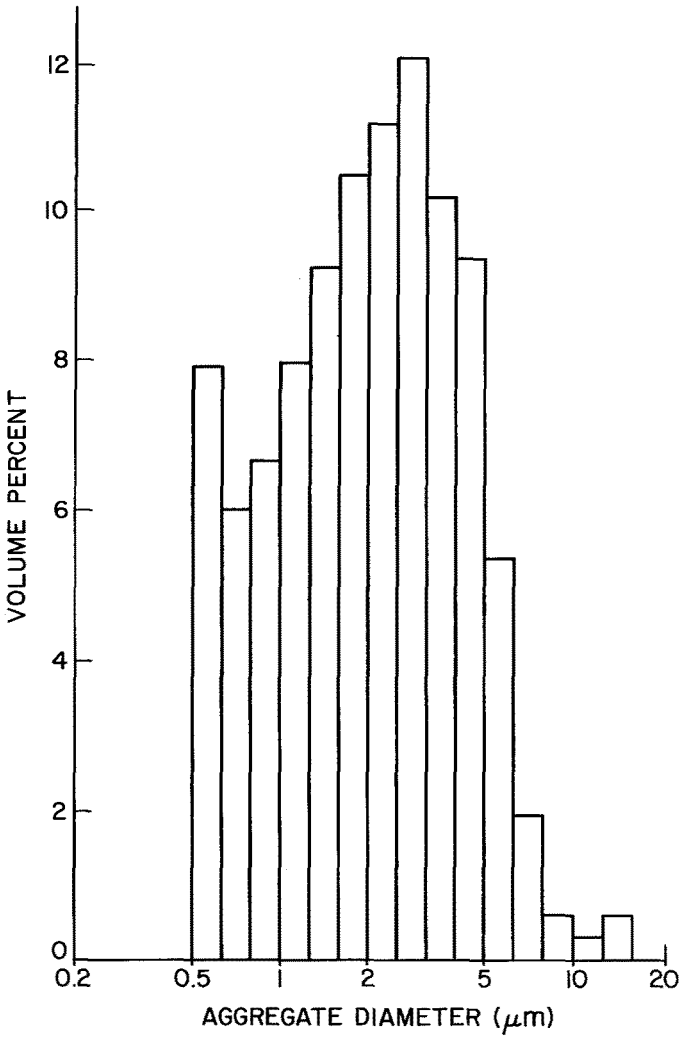

Figure 1 Aggregate size distribution of a sol prepared from 150° C material and milled for 16 h.

exceeds that of the primary peak (at ~ 16 nm) is 62 to 65% and is independent of the material type or time of milling.

Fig. 6 shows the calculated drying shrinkages for the gels. Examples of sintered gel bodies are shown in Fig. 7 for the 900° C material. The diameters of the sintered pieces are in the 6 to 7 mm range. The 150° C material was similarly sintered and showed transparency in all samples except the unmilled pieces sintered at 1300 and 1400°C.

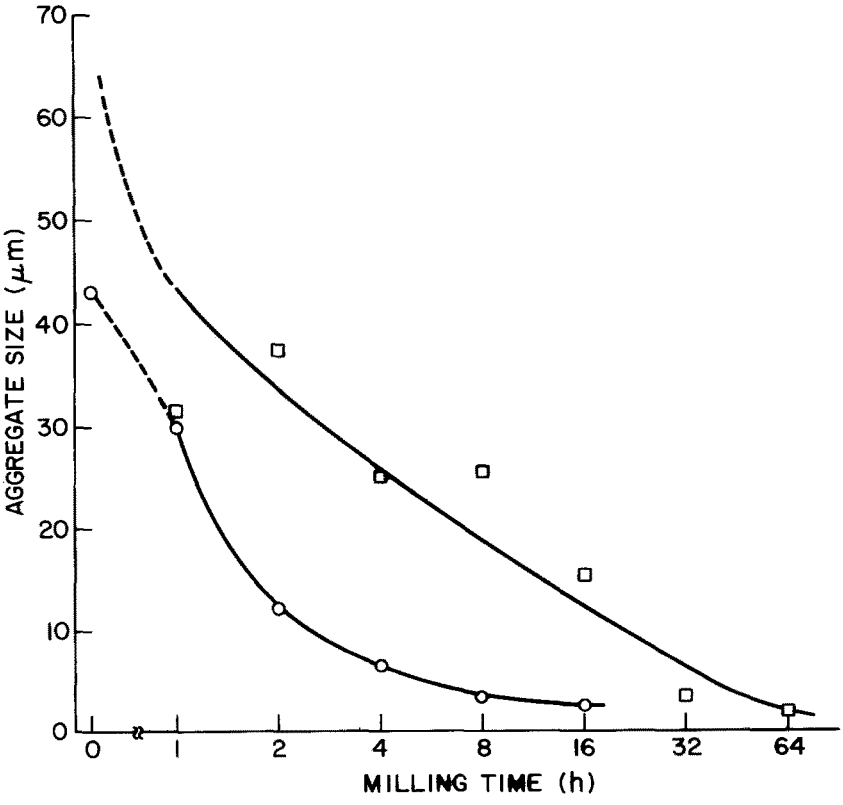

Figure 2 Aggregate size (determined as the peak position from frequency plots such as Fig. 1) plotted against milling time for 150° C (○) and 900° C (□) materials. Note the discontinuous scale to show the aggregate size for the unmilled (zero time) materials. The 900° C material with no milling had aggregates more than 100 μm average size.

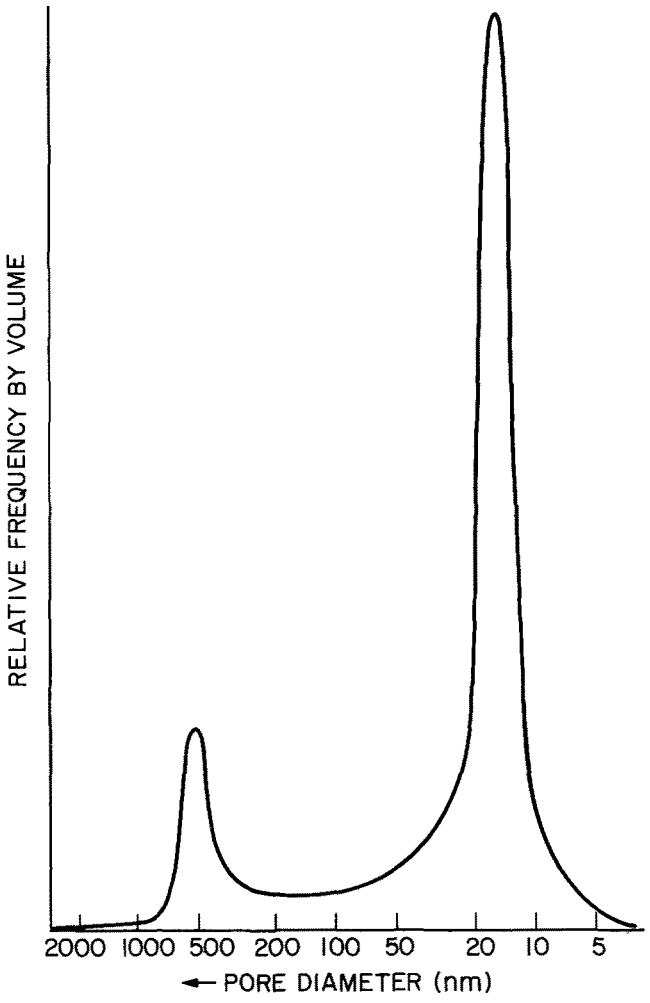

Figure 3 Pore size distribution for a dried gel prepared by milling the 900° C material for 8 h exemplifying both the primary peak due to interparticle spaces and the secondary peak at larger sizes due to interaggregate spaces.

4. Discussion

The aggregate size distribution illustrated in Fig. 1 is nearly a log normal distribution based on the approximate Gaussian shape of a curve generated by connecting the histogram bars when it is noted that the bar at 0.5 μm includes aggregates less than 0.5 μm not measurable by this method. It is important to note from these aggregate size data (Fig. 2) that even after long milling times, the aggregates are much larger than the primary SiO_2 particles from the fumed silica. The fumed SiO_2 has $\sim 200\,m^2\,g^{-1}$ surface area which corresponds to an equivalent spherical diameter of about 14 nm. The smallest aggregate sizes shown in Fig. 2 are approximately 2 μm in diameter; a volume $\sim 3 \times 10^6$ larger than the primary particles. Even considering the packing density of the ultimate particles in the first dried gel which makes up the aggregates, there are $\sim 6 \times 10^4$ particles in a 2 μm aggregate.

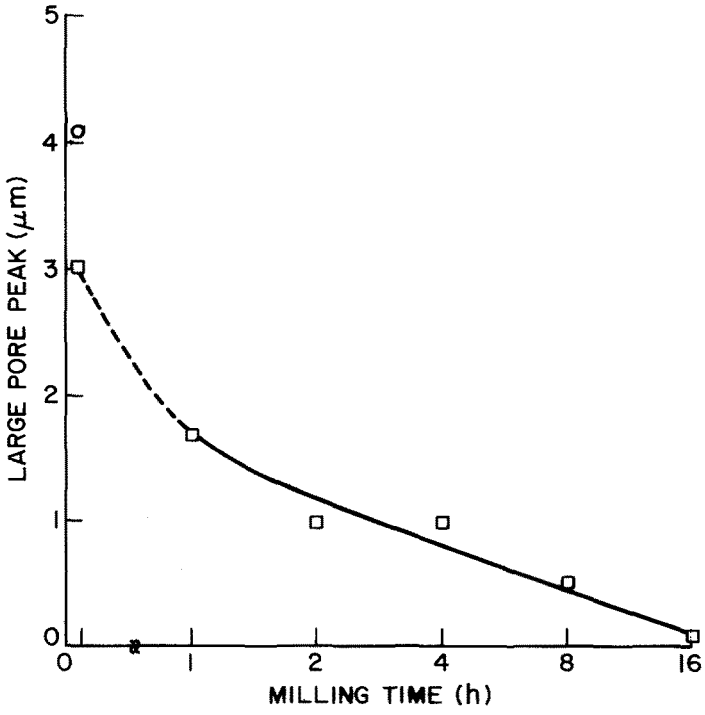

Figure 4 Position of the secondary peaks (determined from data exemplified in Fig. 3) plotted against milling time for the 900° C (□) material. Note the discontinuous scale to show the peak position for the unmilled (zero time) materials. (○ 150° C)

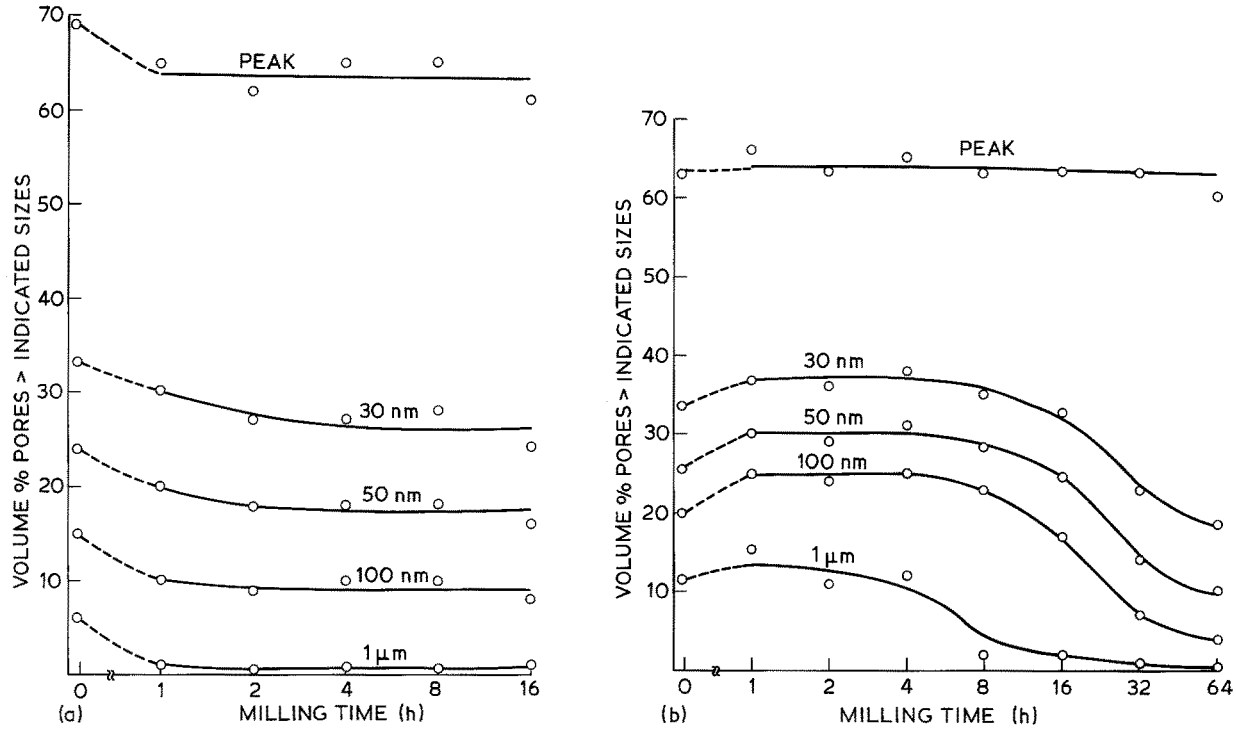

Figure 5 Volume % of pores greater than the peak position for the primary peak at 10 to 16 nm and other selected sizes for (a) the 150° C material and (b) the 900° C material. Note the discontinuous scale to show the data for unmilled (zero time) sols.

The particle sizing instrument used can detect aggregates no smaller than $\sim 0.5\,\mu m$ (2×10^4 ultimate particles) but it is believed that the sol consists of aggregates whose diameters are a continuum of sizes down to the primary particle size of the fumed silica.

The effect of milling time on aggregate size distribution shown in Fig. 2 reveals the expected effect of decreasing aggregate size with increased milling time. Also, the 150° C material, because it is more friable than the 900° C material, shows smaller aggregates at equivalent milling times. Both materials appear to reach a minimum size (for the peak of the distribution) of 2 to 3 μm after extended milling. This is not particularly small when it is realized that hard dense ceramic materials can be milled to less than 1 μm in shorter times. The difference has two causes. First, the viscosity of these sols are often high as a consequence of attempting to maximize the solids loading of the sol. This in turn, reduces the mobility of the balls in the ball jar. Secondly, the SiO_2 milling media has a low density ($2.2\,g\,cm^{-3}$) and are functioning in a fluid of density $1.25\,g\,cm^{-3}$. This decreases the effectiveness of ball–ball or ball–jar collisions.

The pore size distribution in Fig. 3 is typical of those showing bimodal distribution. As expected the position of the primary peak at about 16 nm is nearly independent of the degree of milling and corresponds well to the singular peak observed for once dispersed and dried gels. The peak, therefore, derives from the spaces between the primary particles in the dried gel which makes up the aggregates. The slight asymmetry of this peak (weighted toward larger pores) and the secondary peak at larger pore sizes derives from the spaces between the aggregates. The position of the secondary peak would be expected to move to smaller sizes with increased milling time since the size of the aggregates forming these larger pores have already been shown to decrease with milling (Fig. 2). Indeed this effect is illustrated in Fig. 4. Perhaps, most interesting is the large disparity in the sizes of the aggregates (Fig. 2) and the pores which are hypothesized to be formed by them (Fig. 4). Whereas the size of the pores between the ultimate particles is nearly the same as the diameter of the ultimate particles, the pores between the aggregates are in the order of only 1 to 10% of the size of the aggregates. For example, with 8 h milling of the 900° C material, the primary particle size calculated from specific surface area is 14 nm, approximately equal to the 16 nm size measured for the pores within the aggregates. On the other hand, the measured aggregate size is 25 μm while the secondary peak in the pore size distribution is at 0.5 μm, different by a factor of 50.

The disparity between aggregate sizes and interaggregate pore sizes derives from the interaggregate spaces being filled with yet smaller aggregates in contrast to the primary particles which are of a narrow size distribution and cannot similarly pack into larger pores between primary particles. This distribution of aggregate sizes serving to pack in a fashion giving pores no larger than a few micrometres is useful in that larger pores would present difficulties in removal during sintering.

Also significant in Fig. 4 is the lack of distinct secondary peaks for the 900° C material milled 32 h or longer and for all of the milled 150° C material. In the pore size distributions, this resulted from a merging of the primary and secondary peaks when sufficient milling occurred to reduce the size of the interaggregate pores. That no distinct secondary pore peaks occurred in milled 150° C material indicated the relative ease of aggregate fracture in the 150° C material as opposed to the 900° C material.

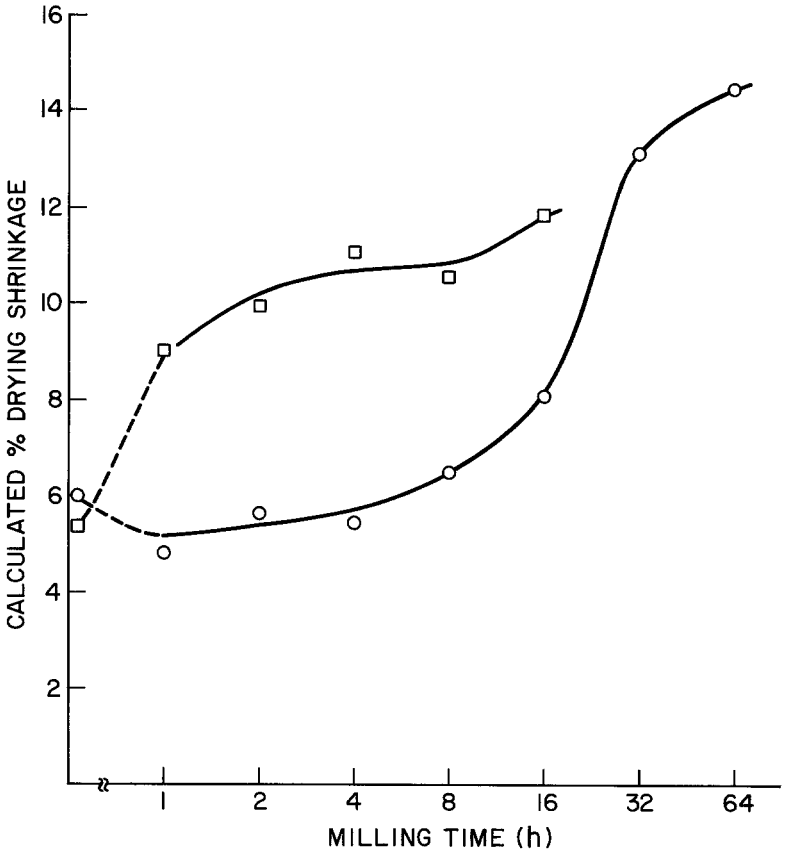

Figure 6 Percentage shrinkage on drying plotted against milling time as calculated from bulk densities of dried gels. Note the discontinuous scale to show the shrinkage of the unmilled (zero time) sols. (□ 150° C material, ○ 900° C material)

When the primary and secondary peaks in the pore size distribution cannot be resolved, a better measure of the effect of aggregates is the asymmetry of the primary peak. This has been represented in Figs 5a and b showing the volume fraction of pores greater than selected sizes as a function of milling time. First, note that for both cases the fraction of pores whose size exceeds that of the highest point on the primary peak (~ 16 nm) is $> 50\%$ illustrating the indicated asymmetry. Also, this fraction is about 62 to 65% and is independent of material type or milling time despite changing aggregate sizes. The shapes of the pore size distribution curves do change with milling time as noted for the curves in Figs 5a and b showing the fraction of pores greater than 30, 50, 100 or 1000 nm. The effect is particularly pronounced in Fig. 5b for the harder 900° C material. Comparing milling times of 2 and 32 h, both have 63 vol % of pores with sizes greater than that of the centre of the primary peak but at the longer milling time this porosity is concentrated in sizes closer to that of the centre of the peak since the fraction larger than, for instance, 1 μm is very small. Thus, with increased milling, the total volume of pores exceeding the size of pores between the primary particles is not decreasing but this constant fraction of larger pores is moved to smaller sizes. Since a log normal distribution of pore sizes predicts that 50 vol % of the pores would be larger than the peak position and since about 62 to 65% are measured to be larger, about 24 to 30 vol % of the pores are accounted for in these larger interagglomerate pores.

One of the principle advantages of this colloidal gel processing using two mixing steps is the ease of drying relatively large parts in times as short as 1 to 2 days without cracking. Part of that ease of drying results from low shrinkage. As has been previously reported [4–6], this low shrinkage results from the aggregates in the sol after the second mixing. In a sol of SiO_2 particles suspended in water, the volume of the sol is essentially unchanged upon gelation. This gel consists of SiO_2 particles bound to each other by hydrogen bonds, perhaps with intermediate coordination sphere H_2O molecules bound between the particles or with weak necks between particles [8]. As the gel dries, the removal of water brings the particles in closer contact and results in shrinkage. It follows then that by introducing aggregates of SiO_2 particles into the sol, the number of shrinkable bonds per unit length decreases and the shrinkage decreases. It also follows that as these aggregates are attrited to smaller sizes, then the shrinkage can be expected to increase. Indeed, this is illustrated in the data shown in Fig. 6.

A successful sol–gel preparation technique requires that the dried gel sinter to a pore free glass. The photograph of the sintered 900° C material in Fig. 7 illustrates well the benefits of the milling procedure. At 1300° C sintering temperature, it was only at the 64 h milling that a highly transparent glass was obtained. At 1325° C the necessary milling time was reduced to 32 h and at 1450° C to 16 h. It should be added that an attempt was made to measure the density of all samples using the immersion technique but the amount of porosity in even the most opaque samples was so small as to be difficult to measure; certainly less than 1 vol %.

Samples of the 150° C material were also sintered at 1300 and 1400° C. While unmilled samples of each did not densify to transparent glass, all of the milled samples did. This part of the study intended to show the effect of milling on very friable aggregates and for this the 150° C material was chosen. In contrast, the 900° C material represents the least friable material that can

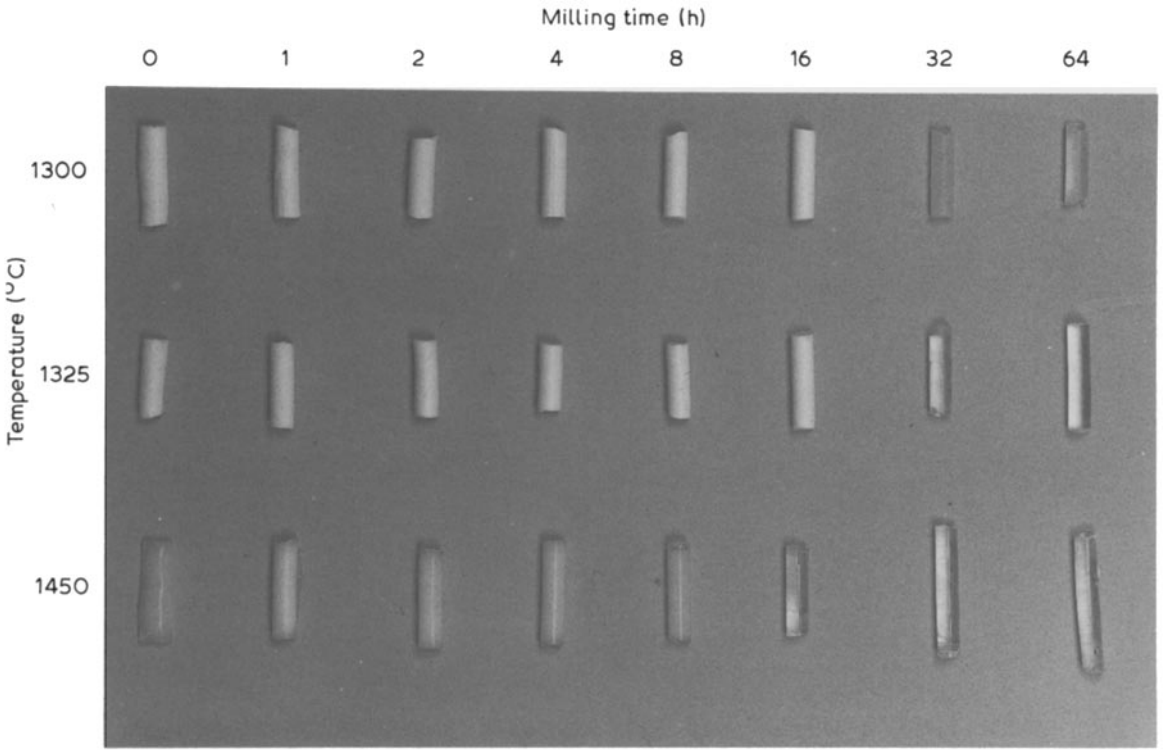

Figure 7 Photograph of sintered glasses prepared from the 900° C material after various milling times and sintering temperatures.

be made while still maintaining the surface area of the original fumed SiO_2. Thus, it follows that less milling is necessary in the 150° C material to obtain optimal transparency than is necessary for the 900° C material.

5. Summary

SiO_2 glasses have been formed by the process of dispersing fumed SiO_2, drying at temperatures of 100 or 900° C and then dispersing the dried aggregates in water to form a sol which can be moulded, dried, dehydrated and sintered. The introduction of an attrition step (ball milling) after the second dispersion had the following consequences.

(1) The average aggregate size decreased from more than 40 μm to less than 3 μm for 16 h milling of the 150° C material and for 64 h milling of the harder 900° C material.

(2) The bimodal pore size distribution for the twice dispersed and dried gels characterized by a primary peak at $\sim$ 16 nm and a secondary peak at 3 to 4 μm is altered by ball milling such that the secondary peak moves toward smaller pore sizes and finally merges into the primary peak.

(3) The volume fraction of pores whose sizes are larger than those in the 16 nm primary peak is always about 24 to 30 vol % regardless of attrition time. The sizes of these larger pores move toward smaller sizes with increased milling to form a shoulder on the primary peak.

(4) The size of the interaggregate pores are more than an order of magnitude smaller than that predicted from an assemblage of aggregates of that particular average size. This is due to the interstities between large aggregates being partly filled with smaller aggregates and particles.

(5) Drying shrinkage increases from about 5 to 6% (linear) to as much as 14% with long milling times.

(6) The more uniform microstructure of gels prepared from milled sols results in higher optical transparency after sintering and allows the elimination of practically all sintering defects.

References

1. L. C. KLEIN, in "Annual Review Materials Science", Vol. 15, edited by R. A. Huggins, J. A. Giordmaine and J. B. Wachtman, Jr (Annual Reviews, Inc. Palo Alto, CA, 1985) pp. 227–248.
2. S. SAKKA, "Treatise on Material Science and Technology," Vol. 22, edited by M. Tomozawa and R. H. Doremus (Academic Press, New York, 1982) pp. 129–167.
3. R. D. SHOUP and W. J. WEIN, US Patent 4059658 November (1977).
4. E. M. RABINOVICH, D. W. JOHNSON, Jr., J. B. MacCHESNEY and E. M. VOGEL, *J. Amer. Ceram. Soc.* **66** (1983) 638–688.
5. D. W. JOHNSON, Jr, E. M. RABINOVICH, J. B. MacCHESNEY and E. M. VOGEL, *ibid.* **66** (1983) 688–693.
6. E. M. RABINOVICH, J. B. MacCHESNEY, D. W. JOHNSON, Jr, J. R. SIMPSON, B. W. MEAGHER, F. V. DiMARCELLO, D. L. WOOD and E. A. SIGETY, *J. Non-Cryst. Solids* **63** (1984) 155–161.
7. G. W. SCHERER and J. C. LUONG, *ibid.* **63** (1984) 163.
8. D. L. WOOD, E. M. RABINOVICH, D. W. JOHNSON, Jr, J. B. MacCHESNEY and E. M. VOGEL, *J. Amer. Ceram. Soc.* **66** (1983) 693–699.

Received 29 February
and accepted 18 July 1988